Development 139, 3221-3231 (2012) doi:10.1242/dev.082800

Integrating force-sensing and signaling pathways in a model for the regulation of wing imaginal disc size

Tinri Aegerter-Wilmsen[1], Maria B. Heimlicher[1], Alister C. Smith[1], Pierre Barbier de Reuille[2], Richard S. Smith[2], Christof M. Aegerter[3] and Konrad Basler[1,*]

SUMMARY

The regulation of organ size constitutes a major unsolved question in developmental biology. The wing imaginal disc of *Drosophila* serves as a widely used model system to study this question. Several mechanisms have been proposed to have an impact on final size, but they are either contradicted by experimental data or they cannot explain a number of key experimental observations and may thus be missing crucial elements. We have modeled a regulatory network that integrates the experimentally confirmed molecular interactions underlying other available models. Furthermore, the network includes hypothetical interactions between mechanical forces and specific growth regulators, leading to a size regulation mechanism that conceptually combines elements of existing models, and can be understood in terms of a compression gradient model. According to this model, compression increases in the center of the disc during growth. Growth stops once compression levels in the disc center reach a certain threshold and the compression gradient drops below a certain level in the rest of the disc. Our model can account for growth termination as well as for the paradoxical observation that growth occurs uniformly in the presence of a growth factor gradient and non-uniformly in the presence of a uniform growth factor distribution. Furthermore, it can account for other experimental observations that argue either in favor or against other models. The model also makes specific predictions about the distribution of cell shape and size in the developing disc, which we were able to confirm experimentally.

KEY WORDS: *Drosophila*, Computer simulations, Growth regulation, Mechanical forces, Wing imaginal disc

INTRODUCTION

Despite considerable research in the area, the issue of how organ size is regulated remains unanswered. A commonly used model system to study this is the wing imaginal disc of *Drosophila*. This is a larval structure that develops into the adult wing during metamorphosis. The size of the wing imaginal disc largely predetermines the size of the final wing (Day and Lawrence, 2000). Disc size appears to be regulated autonomously, as transplants into the female abdomen stop growing when they reach their normal final size (Bryant and Levinson, 1985; Jursnich et al., 1990).

Size regulation is tightly coupled to pattern formation, as major patterning genes are also involved in growth regulation. The most important patterning genes in the wing primordium encode the morphogens Decapentaplegic (Dpp) and Wingless (Wg) (Fig. 1B). Dpp forms a gradient with highest concentrations along the anteroposterior compartment boundary and lowest concentrations in the lateral regions (Basler and Struhl, 1994; Entchev et al., 2000; Posakony et al., 1990; Tabata and Kornberg, 1994; Teleman and Cohen, 2000), whereas Wg forms a gradient perpendicular to the Dpp gradient with the highest concentrations at the dorsoventral compartment boundary (Neumann and Cohen, 1997; Strigini and Cohen, 2000; Zecca et al., 1996) (Fig. 1B). Removing either of these morphogens leads to a severe reduction of wing disc growth (Couso et al., 1994; Neumann and Cohen, 1996a; Ng et al., 1996; Spencer et al., 1982). Notch (N) and Vestigial (Vg) are two other proteins that are involved in both patterning and growth. N is activated at the dorsoventral boundary, where it has been shown to induce growth directly (Baonza and Garcia-Bellido, 2000; Go et al., 1998). Moreover, it promotes growth indirectly by inducing *wg* and *vg* expression (Couso et al., 1995; Diaz-Benjumea and Cohen, 1995; Kim et al., 1995; Klein and Arias, 1998; Rulifson and Blair, 1995). *vg* is regulated by two enhancers, the boundary enhancer (BE) and the quadrant enhancer (QE). BE is induced by N activity, whereas QE is (indirectly) inhibited by the N and induced by the Dpp and Wg signaling pathways (Certel et al., 2000; Kim et al., 1996; Neumann and Cohen, 1996b; Williams et al., 1994; Zecca and Struhl, 2007b) (Fig. 1A). Vg is crucial for the establishment of wing identity and *vg*-null mutants show severely reduced wing disc growth and do not form an adult wing blade (Williams et al., 1991).

Even though it is well established that patterning genes play an important role in growth regulation, it is not known how this is achieved and how growth termination is regulated. Several mechanisms have been proposed in this context.

It has been proposed that a sufficiently steep morphogen concentration gradient induces growth (Bohn, 1976; French et al., 1976). For the wing disc, it has been proposed that the Dpp gradient plays such a role (Day and Lawrence, 2000; Rogulja and Irvine, 2005), and is involved in size regulation (Day and Lawrence, 2000). In the most basic model, it is assumed that the Dpp concentrations are fixed at the anteroposterior boundary and at the most lateral edge of the disc. During growth, the Dpp concentration gradient decreases. Growth stops once the magnitude of the gradient drops below a specific threshold value (Day and Lawrence, 2000). On a molecular level, there is evidence suggesting that the Dpp gradient is converted into opposing gradients of Four-jointed (Fj) and Dachsous (Ds) (Rogulja et al., 2008). Concentration differences of Fj and Ds have, in turn, been shown to control the growth regulating hippo pathway by changing the intracellular localization of the atypical myosin Dachs (D). This then leads to activation of the protein Yorkie (Yki),

[1]Institute of Molecular Life Sciences, University of Zurich, CH-8057, Switzerland. [2]Institute for Plant Science, University of Bern, CH-3013, Switzerland. [3]Institute of Physics, University of Zurich, CH-8057, Switzerland.

*Author for correspondence (basler@imls.uzh.ch)

Accepted 7 June 2012

which results in the induction of growth (Rogulja et al., 2008; Willecke et al., 2008). Even though there is strong evidence in favor of aspects of this model, there are also data contradicting the proposed essential roles of the Dpp concentration gradient in establishing Fj and Ds gradients (Schwank et al., 2011) and in growth regulation (Schwank et al., 2008).

It has also been proposed that a Vg feed-forward mechanism has a large impact on final size. As described above, one of the *vg* enhancers, QE, is activated by Wg and Dpp. It has been shown, however, that these factors are not sufficient, but that QE is activated when, in addition, *vg* is expressed in neighboring cells (Zecca and Struhl, 2007b). As for the induction of growth by the Dpp gradient, this mechanism has been shown to act via the Hippo pathway (Zecca and Struhl, 2010). This Vg feed-forward mechanism appears to have a large effect on the expansion of the wing primordium (Zecca and Struhl, 2007a), but it has not yet been included into a model for final size regulation.

Mechanical forces have also been proposed to play a role in growth regulation (Shraiman, 2005) and wing disc size regulation (Aegerter-Wilmsen et al., 2007; Hufnagel et al., 2007). In these models, it is proposed that compression inhibits growth, and increases in the center of the wing disc during growth. Growth is terminated once the stimulatory effect of growth factors in the center of the disc can no longer overcome the inhibitory effect of mechanical compression. The role of mechanical forces in growth regulation has not yet been tested directly; however, there is some indirect evidence in favor of this hypothesis (Aegerter-Wilmsen et al., 2010; Nienhaus et al., 2009). Even though, to our knowledge, the mechanical force models have not been contradicted by data, alone they cannot explain several observations that are used to support the other proposed mechanisms and thus the models may be missing crucial elements for final size determination.

Here, we formulate a regulatory network of experimentally confirmed interactions, including the main components underlying the Vg feed-forward mechanism and the Dpp gradient model. In addition, we have added hypothetical interactions of specific network components with mechanical forces. We show that, as an emergent behavior of the regulatory network, different aspects of growth dynamics are reproduced. Furthermore, the network can reproduce a set of key experimental results that have been used to support or refute other existing models. Our model makes specific predictions about the distribution of cell shape and size in the developing disc. In order to test our predictions, we have developed a technique for analyzing cell geometry on the curved surface of the wing disc. We find that our data are in agreement with the predictions of the model.

MATERIALS AND METHODS

Modeling

The modeling program consists of two parts that interact with each other. One part governs interactions within the regulatory network, the other governs changes in polygonal cell shapes.

The regulatory network (Fig. 1A) has two different types of inputs: protein activity profiles of a selection of patterning genes (Fig. 1B; supplementary material Table S1) and mechanical compression. A measure for compression is calculated based on a weighted average of the area of a cell and its surroundings (supplementary material Table S1). Equations governing the protein activities in the network in the wild-type situation and in the different simulated mutants can be found in supplementary material Tables S2 and S3, respectively.

The network has two outputs that are relevant for the cell shape calculation part. The most important output concerns the growth rate, the rate at which a cell progresses through its cell cycle. Once a cell reaches the end of the cycle, it divides. The growth rate (% cell cycle progression/hour) for the αth cell is calculated as follows:

$$G_\alpha = (cg1 + cg2*[Yki]_\alpha + cg3*[Vg]_\alpha + cg4*[N]_\alpha - cg5*[Brk]_\alpha)*cg6\ , \quad (1)$$

where $cg1$=–12%/hour, $cg2$=8%/hour, $cg3$=6%/hour, $cg4$=2%/hour, $cg5$=7%/hour, $cg6$=0.048 and $[Protein]_\alpha$=concentration of active protein normalized for maximum N, and where it is assumed that the effect of *Vg* on growth is satisfied for normalized levels higher than 1. We have set Δt to be equal to the time that is required to go through mitosis (~20 minutes), so that the simulation should show the same percentage of mitotic cells as a still image of a growing disc. BrdU staining was simulated by marking cells as soon as they completed 70% of the cell cycle. This marking was retained for three consecutive time steps (corresponding to about 1 hour simulated time). The growth constant $cg6$ was fitted in such a way that the minimum cell cycle time corresponds to roughly 6 hours. It is assumed that progression through the cell cycle does not affect cell shape directly, as no correlation has been found between cell volume and apical cell areas (Aegerter-Wilmsen et al., 2010), which is modeled here. Therefore, the relevant output of the regulatory network is in fact the identity of cells which divide at a certain time point.

The second output of the network concerns the asymmetric D localization, which is used as a factor that induces a bias in the direction of the cell division plane. If [D] is larger than 0.1, the bias is implemented and the angle of the division plane is equal to the mean of a randomly chosen angle and the angle of a vertex perpendicular to the direction of the Ds/Fj gradient ([Xgradw,Ygradw] (supplementary material Table S2).

Cell division brings the tissue out of mechanical equilibrium. New apical cell shapes are found by using a vertex model, which assumes cell shapes to be polygonal (Farhadifar et al., 2007; Hufnagel et al., 2007). It defines the shape of a cell by the positions of its vertices, i.e. the positions where three cell sides (edges) meet. Cell shapes are calculated by minimizing the following energy function using a conjugate gradient method:

$$E(R_i) = \sum_\alpha \tfrac{K_\alpha}{2} * (A_\alpha - A_\alpha^{(0)})^2 + \sum_{<i,j>} \Lambda_{ij} l_{ij} + \sum_\alpha \tfrac{\Gamma_\alpha}{2} * L_\alpha^2\ . \quad (2)$$

The meanings of the terms and parameters are as previously described (Farhadifar et al., 2007). In contrast to earlier implementations (Aegerter-Wilmsen et al., 2010; Farhadifar et al., 2007), we do not use periodic boundary conditions, thus not imposing any limitations on the development of overall disc shape. For non-boundary cells, we use parameter values that correspond to case I of Farhadifar et al. (Farhadifar et al., 2007), where cells are identical and $\Gamma' = \Gamma/(KA^{(0)}) = 0.04$ (–) and $\Lambda' = \Lambda/(KA^{(0)3/2}) = 0.12$ (–). For boundary cells, Λ' was set to 0.09 (–). In order to prevent some artifacts arising from an irregular boundary, it was smoothened by multiplying the growth rates of its cells by 0.7. Upon energy minimization, new cell areas serve as input for the regulatory network. The simulated disc generally contains 36 hexagons initially and is allowed to grow until 100 hours have been simulated.

Experiments

Phenotypic wild-type discs were dissected from larvae with genotypes *y, w, hs-flp; wg-lacZ/CyO* or *y. w, hs-flp; Sp/CyO;vg-QE-lacZ*. Wing discs were fixed and prepared for immunocytochemistry using standard procedures. Primary antibodies used were chicken anti-β-galactosidase (ICL, Portland, OR, USA, 1:1000) and mouse anti-Dlg (Developmental Studies Hybridoma Bank, Iowa City, IA, USA, 1:200). Secondary antibodies were Alexa 594 goat-anti-chicken IgG and Alexa 488 goat-anti-mouse IgG (Molecular Probes, Grand Island, NY, USA, 1:400 and 1:200, respectively).

Cell shape analysis

Cell shapes were extracted from the curved pouch using MorphoGraphX (Kierzkowski et al., 2012) (supplementary material Fig. S1) and analyzed with respect to their relative distance from the center. In order to compensate for curvature, we used polygonal fitting in combination with line integration. Elongation was calculated according to Asipauskas et al.

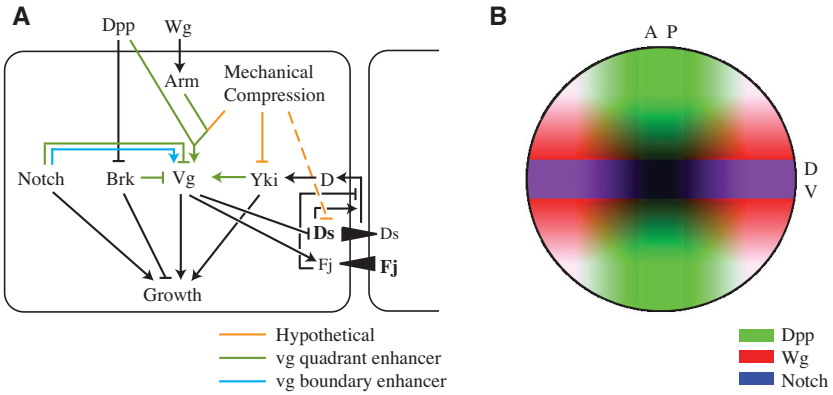

Fig. 1. Main assumptions underlying the model. The regulatory network (**A**) represents protein activities and interactions that regulate these activities. The model does not distinguish between interactions at the transcriptional and protein activity level, but considers effects on net activities. All protein activities emerge from the network, except for those of Dpp, Wg and N, which are implemented in the model as depicted in **B**. In the regulatory network, differences in Ds and Fj concentrations between neighboring cells lead to activation of D by changing its intracellular localization. For simplicity, the resulting asymmetric localization is not depicted. In addition to the assumptions shown, it is assumed that apical cell shapes can be found by minimizing Eqn 2, that a weighted average of the area of a cell and its neighbors is a good readout for mechanical stress, that cells do not rearrange when exposed to mechanical tension, and that the planar polarization of D imposes a bias on the direction of the division plane. The interactions shown in orange are hypothetical and form the main untested assumptions underlying the model. The regulation of *ds* by mechanical compression is dotted, as this regulation is not essential for the principle behind size regulation in the model, but improves the fit of simulation results with experimental data. AP, anteroposterior boundary; DV, dorsoventral boundary. All discs in this paper have the same orientation as in B.

(Asipauskas et al., 2003). Curvature was compensated for in such a way that elongation along the *z*-axis was integrated into radial elongation. Mitotic cells were selected based on their size.

RESULTS

Assumptions

The assumptions underlying the model are depicted in (Fig. 1). The model is formulated for the wing pouch, which eventually develops into the wing blade. The regulatory network contains the major growth regulators that closely interact with patterning. This is because we aimed to reproduce the principle underlying size regulation and considered it to be likely that such components are essential for this principle, in contrast to factors that modulate growth rates in all cells to a similar extent.

Protein activity levels in the model result from the interactions within the network (Fig. 1A), except for those of N, Dpp and Wg, which are implemented directly (Fig. 1B). The Dpp gradient is assumed to adjust to the dimensions of the disc, whereas the Wg gradient is assumed to be fixed, in agreement with experimental observations (Teleman and Cohen, 2000). These assumptions about scaling, however, are not relevant for the principle behind growth termination in the model.

All regulatory interactions in the signaling network have been confirmed experimentally (Baonza and Garcia-Bellido, 2000; Campbell and Tomlinson, 1999; Go et al., 1998; Goulev et al., 2008; Halder et al., 1998; Huang et al., 2005; Jazwinska et al., 1999; Kim et al., 1997; Kim et al., 1996; Kirkpatrick et al., 2001; Mao et al., 2006; Martín et al., 2004; Minami et al., 1999; Neumann and Cohen, 1996b; Rogulja et al., 2008; Willecke et al., 2008; Williams et al., 1991; Williams et al., 1994; Zecca and Struhl, 2007a; Zecca and Struhl, 2007b; Zecca and Struhl, 2010), except for those concerning mechanical forces (drawn in orange in Fig. 1A). The first hypothetical interaction concerns the regulation of Armadillo (Arm) by compression. Arm has been shown to be activated by compression in the *Drosophila* embryo (Desprat et al., 2008; Farge, 2003), but this has not been tested for the wing disc.

The second hypothetical interaction concerns the regulation of Yki activity by mechanical forces. Very recently, this interaction has been shown to occur in mammalian cells (Dupont et al., 2011; Wada et al., 2011). There are some indirect indications that this regulation might also occur in the wing imaginal disc. First, it has been found that modulating F-actin organization, which may affect the mechanical forces exerted by cells, leads to changes in Yki activity (Fernández et al., 2011; Sansores-Garcia et al., 2011). Second, Zyxin has been identified as an upstream regulator of Yki in the wing disc (Rauskolb et al., 2011), and this protein has previously been shown to change its intracellular localization upon exposure to mechanical tension in mammalian cells (Lele et al., 2006; Yoshigi et al., 2005). There is also some evidence suggesting that Zyxin reacts to forces in the *Drosophila* embryo (Colombelli et al., 2009).

The third hypothetical interaction concerns the inhibition of *ds* expression by mechanical forces. Such a link has not yet been shown to our knowledge. We note that this hypothesis is not essential for the principle behind growth termination in the model, but it improves the results. For example, the expression patterns of *vg* and *ds* are not completely complementary in the wing disc (Rodríguez, 2004), but they would be in our model if *ds* is only regulated by Vg. It would in principle also be conceivable that *ds* is regulated, for example, by a protein that is active in a ring surrounding the pouch.

In the regulatory network, differences in Ds and Fj concentrations between neighboring cells are assumed to activate Yki via D, as has been shown experimentally (Rogulja et al., 2008; Willecke et al., 2008; Zecca and Struhl, 2010). Large differences in Ds and Fj concentrations appear to be detected over several cell diameters (Willecke et al., 2008). Therefore, a weighted average of the gradient sensed by a cell and its neighbors was used in the model.

In addition to the signaling network, the model also makes assumptions with respect to the mechanical properties of cells. It assumes that apical cell shapes can be well described by

minimizing an energy function that was developed by Farhadifar et al. (Farhadifar et al., 2007) and that was fitted to different experimental data on the wing disc. This implies constant and identical mechanical properties across cells. Furthermore, it assumes that the cell area is a good readout for mechanical stress in such a model. Moreover, it assumes that the average mechanical stress present in a region also influences individual cells. This is because it has been shown that several components of the contracting actin-myosin network are recruited by mechanical stress (Kasza and Zallen, 2011). In addition, it assumes that cells do not rearrange, i.e. that they do not change neighbor contacts in response to tension. This assumption is supported by the general observation of contiguous cell lineage clones (Resino et al., 2002), the absence of large-scale sorting and rearrangements upon visual inspection of movies of growing wing discs, and the maintenance of neighbor connections during mitosis, despite the associated profound changes in apical cell shape (Gibson et al., 2006). Last, it is assumed that the direction of the division plane is influenced by the asymmetric intracellular localization of D, as has been shown experimentally (Mao et al., 2011).

For simplicity, the wing pouch is modeled as a flat tissue, even though it becomes folded towards the end of growth. The model fully integrates the Vg feed-forward mechanism, even though it does not explicitly include Vg autoregulation or the protein Fat (Ft), an upstream regulator of the Hippo pathway, which has been shown to be essential for sending the feed-forward signal. These components have been left out of the model for simplicity, but can be added without any quantitative consequences.

Size regulation mechanism

The hypothetical interactions in Fig. 1A were not only added based on analogies in other tissues, but also in order to create a network that can account for growth termination. The envisioned size regulatory mechanism conceptually combines elements from existing models (Aegerter-Wilmsen et al., 2007; Day and Lawrence, 2000; Hufnagel et al., 2007) and can be understood in terms of a compression gradient model. Compression builds up in the center, where growth ceases once the compression level reaches a certain threshold. In the rest of the disc, growth ceases when the compression gradient drops below a certain threshold level (Fig. 2A).

On a molecular level, the following is proposed to occur in the center of the disc (Fig. 2B). Initially, the combined activity of growth factors is highest in this region. The negative regulator Brinker (Brk) is absent and the positive regulators Vg and N are present. Furthermore, no compression has built up yet, so that the activity of the positive growth regulator Yki is relatively high. As the combined growth factor concentration is highest in the center, this region will initially grow faster than the surrounding regions. As long as the disc stays flat, this will lead to a build up of compression in the center, which causes a decrease in Yki activity. When Yki levels become too low, the combined activity of Vg and N is no longer sufficient to induce growth.

Because of the initial build up of compression in the center of the disc, the regions adjacent to the center become exposed to a steep compression gradient. This is proposed to induce growth via the following mechanism (Fig. 2C): *vg* is assumed to be induced by a compression-dependent mechanism, whereas *ds* is assumed to

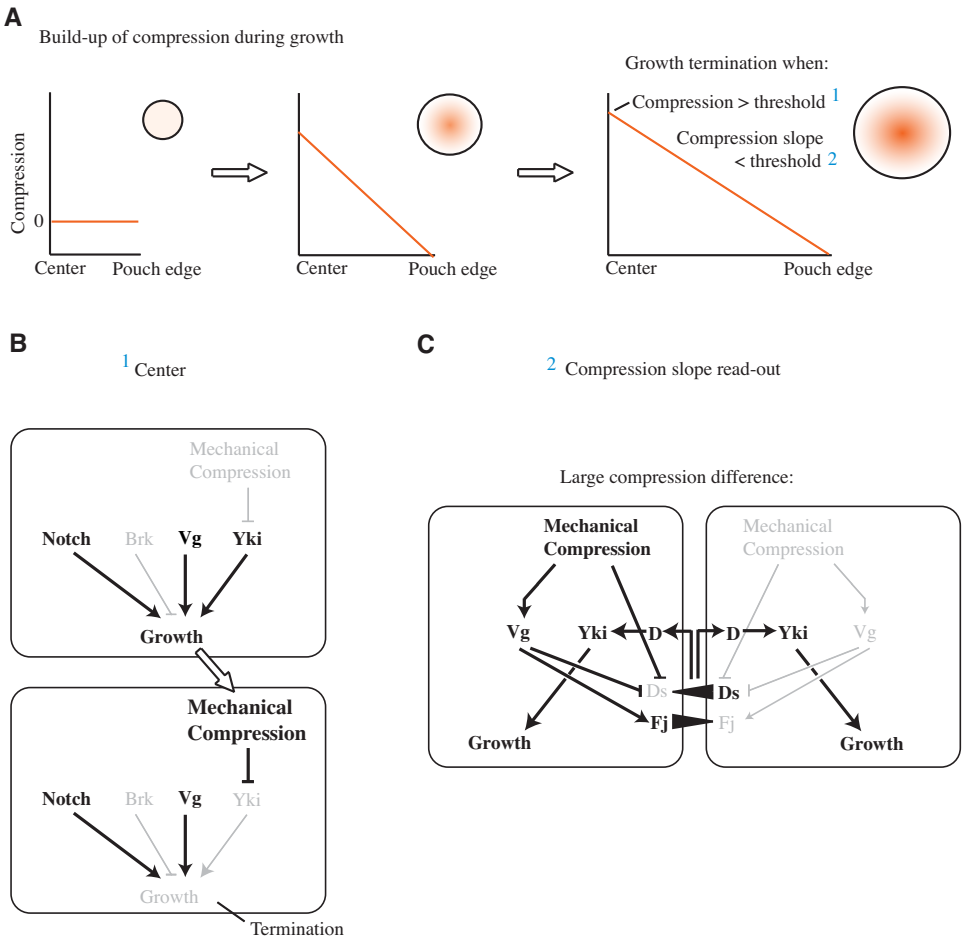

Fig. 2. The size regulation mechanism can be understood in terms of a compression gradient model. (**A**) General principle: compression increases in the center during growth. Growth ceases when compression is higher than a certain threshold in the center and the compression gradient is lower than a threshold level in the rest of the disc. (**B**,**C**) The situations in the center and periphery are depicted in more detail in B and C, respectively. This explanation only involves part of the model and is thus a simplification of the size-regulating mechanism.

be inhibited by compression. Therefore, a steep compression gradient will result in a steep Vg gradient and an opposing steep Ds gradient. As Vg induces *fj* and inhibits *ds*, the steep Vg gradient then leads to a steep Fj gradient and it further increases the slope of the Ds gradient. The opposing Fj and Ds gradients cause an asymmetric intracellular localization of D, which induces growth via the activation of Yki. Growth ceases when the compression gradient is too shallow to activate sufficient Yki for growth induction.

The above explanation involves only part of the network and the size-regulating mechanism in the model is more complicated. For example, the Vg-QE activation pattern is not only influenced by the distribution of mechanical stress, but also by the presence of Vg in the dorsoventral boundary and the distribution of Wg and Dpp. The precise effects of the different growth regulatory mechanisms are position and time dependent, and are also somewhat influenced by the exact parameter values used.

Comparison of modeling results with available data

We aimed to reproduce the most important dynamics of the system as well as a number of key experimental results that are used to argue for and against existing models. In the following section, we focus on these features.

Growth dynamics

The model was developed in order to explain wing disc size regulation. The most important feature it should therefore be able to reproduce is the large increase in cell cycle time, which has been observed experimentally (Bryant and Levinson, 1985). In the wing disc, growth first occurs roughly exponentially and then slows down (Bittig et al., 2009). The model generates the growth curve as shown in Fig. 3A. Indeed, an exponential growth phase is followed by a large decrease in growth rates. The cell number doubling time increases from about 6 to about 150 hours, and the mitotic index decreases from about 6 to about 0.5%, in agreement with the experimental data (Bryant and Levinson, 1985; Wartlick et al., 2011). The decrease in growth rates in the model is predominantly caused by decreased Yki activity, as a result of increasing absolute compression levels and a decreasing compression gradient.

It has been observed that growth occurs roughly uniformly throughout the disc, even though Dpp, one of the main growth factors, is present in a gradient (Milán et al., 1996; Schwank et al., 2011). Our model seems to yield roughly uniform growth in the presence of the Dpp gradient (Fig. 3C; supplementary material Movie 1). We also quantified medial and lateral growth using an approach similar to that employed by Schwank et al. (Schwank et al., 2008), and found that there is no significant difference in growth rates between these regions (P=0.2; Fig. 3B). There are several feedback mechanisms responsible for the roughly uniform growth: increased growth leads to increased compression, which decreases growth, and it leads to a compression gradient that induces growth in regions with lower growth rates.

Growth in a disc with experimentally induced uniform Dpp shows a non-uniform growth pattern, with high rates laterally and low rates medially (Rogulja and Irvine, 2005; Schwank et al., 2008). Our model reproduces this pattern (Fig. 3D; supplementary material Movie 2). Quantification shows that the growth rates are indeed

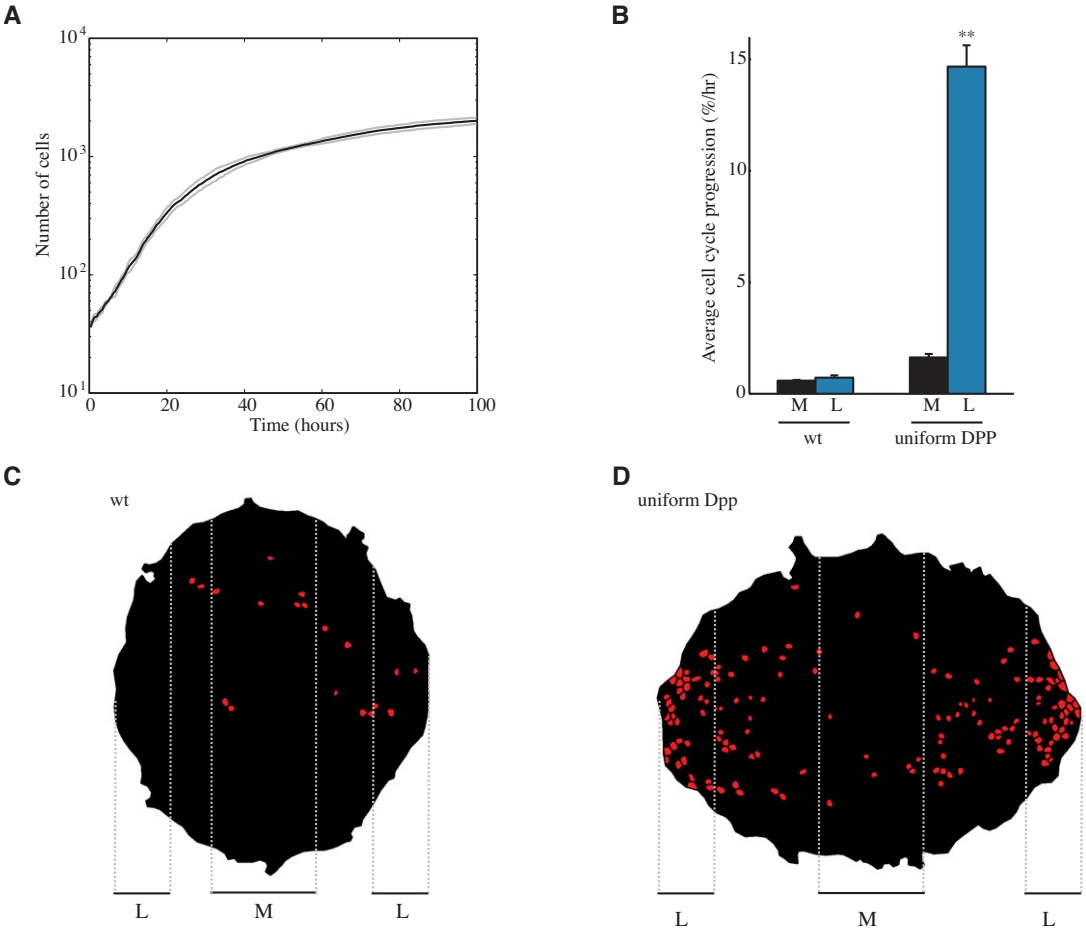

Fig. 3. Simulation data on growth dynamics. (**A**) The average growth curve is depicted in black, whereas the average growth curve ±s.d. is depicted in gray. (**B**) Quantification of growth rates (±s.e.m.) in the lateral (L) and medial (M) parts of simulated wild-type discs and discs with uniform Dpp signaling, respectively. Different time points are used for analysis, as the discs with uniform Dpp grow considerably faster than wild-type discs. *P* values were obtained with a two-sided Student's *t*-test; $^{**}P<0.005$. (**C**,**D**) Simulated BrdU staining in wild-type discs and discs with uniform Dpp signaling. The indicated definitions of the lateral and medial regions were used for the quantification in B.

significantly different (P<0.005; Fig. 3C), as has been found experimentally (Schwank et al., 2008). Similar results are obtained here for a *brk*-null mutant and for a *dpp*, *brk* double mutant (data not shown), also in agreement with existing data (Schwank et al., 2008).

It has been shown experimentally that medial growth rates decrease when uniform Dpp signaling is induced (Rogulja and Irvine, 2005; Schwank et al., 2008). However, medial growth levels are higher in the simulated disc with uniform Dpp signaling than in the simulated wild-type disc in Fig. 3B. This is partly because discs with different simulated ages are used, as discs with uniform Dpp signaling grow much faster than wild-type discs. In order to test whether uniform Dpp signaling decreases medial growth, we induced Dpp signaling during growth and compared growth levels before and after induction. In this case, medial growth levels did not change significantly (1.4% cell cycle progression/hour before versus 1.5%/hour after induction; P=0.1). Lateral growth levels still increased (from 1.7 to 13.2%/hour; P<0.005). A possible explanation for this discrepancy will be discussed below (see Discussion).

The shapes of clones also give some information about growth dynamics. In the wild-type wing disc, clones are elongated along the proximodistal axis (Baena-López et al., 2005; Mao et al., 2011). A similar orientation is seen in our simulations (supplementary material Fig. S2).

Experiments related to the Dpp gradient model

A key experiment that has been used to argue in favor of the Dpp gradient model concerns the non-autonomous growth induction by clones in which Dpp signaling is increased (Rogulja and Irvine, 2005). As can be seen in Fig. 4A, the model reproduces this observation. Contrary to expectation of the Dpp gradient model, it has also been shown that this growth-inducing effect is transient (Rogulja and Irvine, 2005). In our model, the growth-inducing effect is transient (compare Fig. 4A with 4A′). Non-autonomous growth induction in the model is the consequence of a boundary effect caused by increased Vg activity within the clones. This effect is transient due to negative effects of increased compression resulting from additional growth.

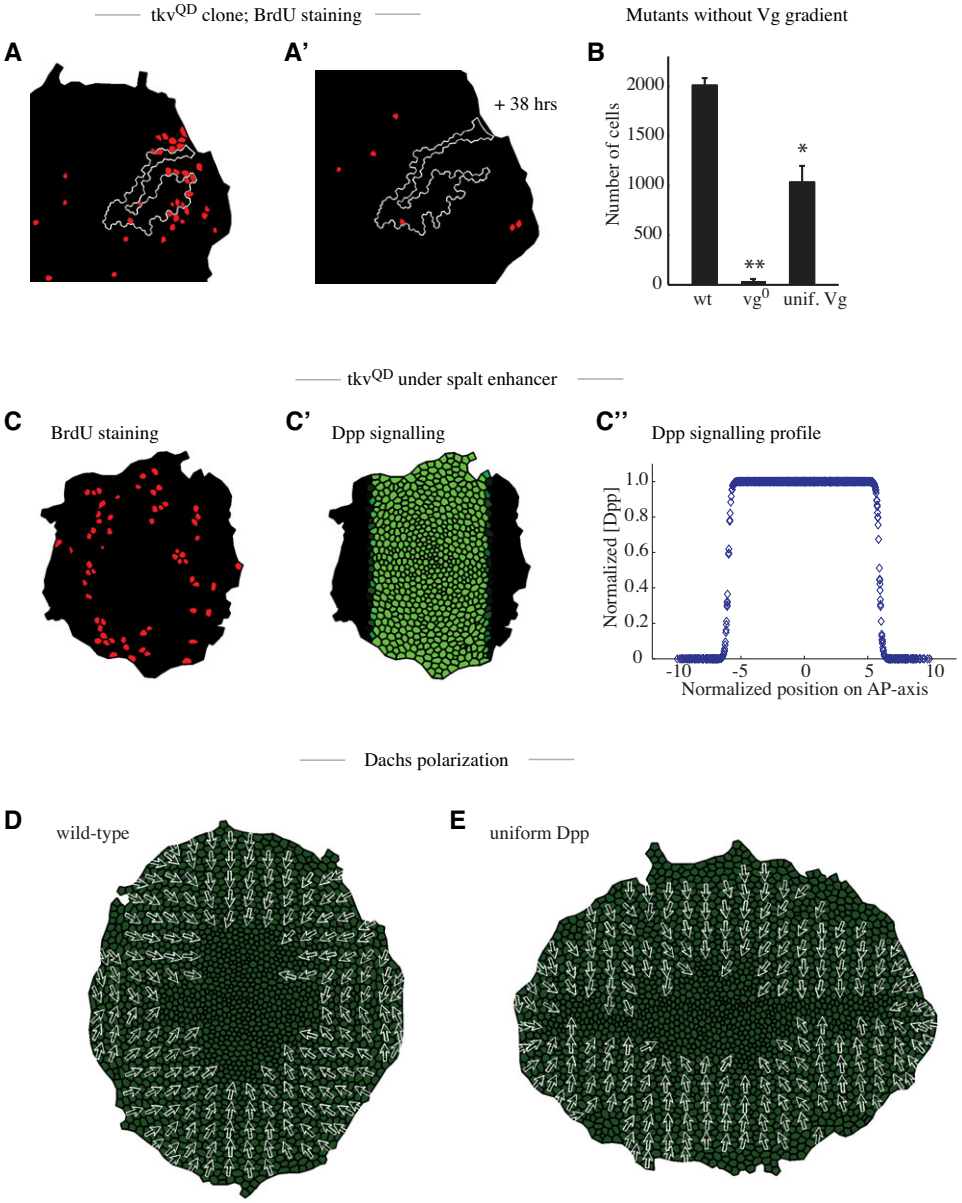

Fig. 4. Simulation results of experiments related to the Dpp gradient model. (**A**) A steep Dpp gradient is created by introducing high levels of Dpp signaling inside the clone. The same simulation is shown at a later time point (**A′**). (**B**) Comparison of final sizes in the wild type, a *vg*-null mutant and a mutant with high uniform levels of Vg (±s.e.m.). *P* values were obtained with a two-sided Student's *t*-test; *P<0.01, **P<0.0001 compared with wild type. (**C-C″**) Simulation of an experiment where tkv^{QD} was expressed under the *spalt* enhancer by creating a Dpp profile as shown in C′ and C″. (**D**,**E**) The polarized intracellular localization of D in wild type and discs with uniform Dpp signaling, respectively. The arrows indicate the average directions of D polarization for small groups of cells. Arrows are included only if the polarization is sufficiently pronounced ($(\langle Xgradw\rangle^2+\langle Ygradw\rangle^2)^{0.5}$>0.15, see supplementary material Table S2). Clones in this and other figures are outlined in white.

In favor of the gradient model, it has also been shown that disc size is decreased when the gradient of *vg*, which is a target of Dpp, is decreased by either overexpressing (saturation of response) or deleting *vg* (Baena-Lopez and García-Bellido, 2006; Williams et al., 1991). In agreement with the experimental data, growth does not occur in a *vg*-null mutant in our model and is decreased in discs with uniform vg overexpression (Fig. 4B).

As further support for the Dpp gradient model, it has been shown that boundaries of Ds and Fj activity lead to growth induction (Rogulja et al., 2008; Willecke et al., 2008). As can be expected from the assumptions underlying our model, induction of either *ds* or *fj* in clones also leads to growth induction at the clone boundaries (supplementary material Fig. S3).

As mentioned above, uniform Dpp signaling leads to increased lateral growth (Rogulja and Irvine, 2005; Schwank et al., 2008), which contradicts an essential role for a Dpp signaling gradient in these lateral regions. In order to study the role of a Dpp signaling gradient in the medial part of the disc, an activated form of the Dpp receptor Thickveins, Tkv^{QD}, was expressed under the spalt enhancer, which is activated by high levels of Dpp pathway activity (Schwank et al., 2008). Such Tkv^{QD} expression leads to the complete repression of *brk* in the medial region and thus to a flat Brk profile (Schwank et al., 2008). As it has been shown that Dpp regulates growth exclusively via Brk (Schwank et al., 2008), it would be predicted that growth is eliminated in the medial part of the disc if Dpp signaling differences are required for growth induction. However, growth was found to occur in this region, showing that a gradient of Dpp signaling is also not essential for medial growth induction (Schwank et al., 2008). This experimental outcome is reproduced by our model (Fig. 4C).

It has been proposed that graded Dpp activity induces growth by influencing asymmetric subcellular D localization (Rogulja et al., 2008). However, this polarization is not strongly altered in mutants with uniform Dpp signaling, which would have been expected based on this hypothesis (Schwank et al., 2011). Our model reproduces the observed proximodistal polarization of D, as well as the somewhat shifted polarization pattern in discs with uniform Dpp signaling (Mao et al., 2006; Rogulja et al., 2008; Schwank et al., 2011). It also reproduces the absence of clear polarization in the centers of these discs (Fig. 4D,E).

Experiments related to the Vg feed-forward mechanism

The ability of Vg to induce its expression in neighboring cells has been shown most clearly by the following set of experiments (Zecca and Struhl, 2007b): first, vg-QE activity was measured in discs that are mutant for *apterous* (*ap*). In these mutants, the dorsoventral boundary is not formed and N is not activated (Couso et al., 1995; Diaz-Benjumea and Cohen, 1995; Williams et al., 1993). Consequently, *vg-BE* is not induced and *wg* expression is largely reduced. Furthermore, *vg-QE* is not activated and the pouch does not grow (Zecca and Struhl, 2007b). When uniform *wg* expression is induced, Vg is still absent, showing that Wg (and Dpp present in these discs) are not sufficient to induce *vg-QE*. However, when a clone is induced to express *vg*, *vg-QE* is activated autonomously, as well as non-autonomously, in a position-dependent manner and the pouch is partially restored (Zecca and Struhl, 2007b). Our model reproduces these results (Fig. 5).

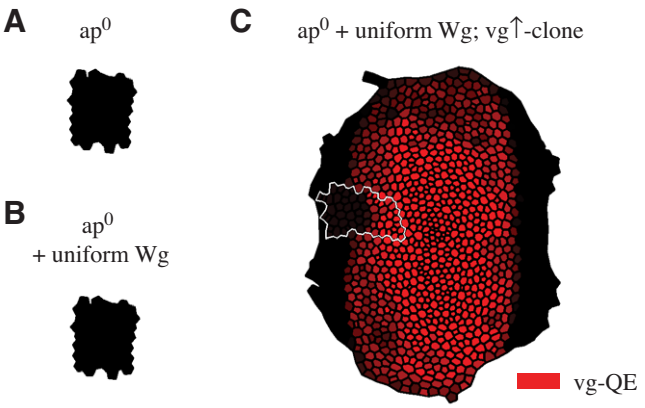

Fig. 5. Simulation results of experiments related to the Vg feed-forward mechanism. (**A**) For the simulation of the *ap* mutant, N is removed and Wg levels are assumed to be constant at a low level. Because of the absence of N, no Vg is produced via the BE either. (**B**) Uniform high levels of Wg were added. In this case, all previously known regulators of *vg-QE* are present, except for *vg* expression in neighboring cells. (**C**) A clone with intermediate Vg levels is added that does not produce additional Wg.

Experiments related to the mechanical force models

In support of mechanical force models, it has recently been shown with birefringence measurements that compression in the center of the disc correlates with disc size (Nienhaus et al., 2009). In discs with uniform Dpp signaling, compression also becomes high in the center, but more ridge shaped (Nienhaus et al., 2009). The model reproduces these results (supplementary material Fig. S4A; see also Fig. 6A,B,C).

Apical cell shapes in the wing disc epithelium resemble polygons with different numbers of neighbors. The polygon distribution was measured for the entire cell population as well as for mitotic cells only (Aegerter-Wilmsen et al., 2010; Farhadifar et al., 2007; Gibson et al., 2006). These data had been reproduced only using models that contain a growth regulatory role for mechanical forces, which argued in favor of such a role (Aegerter-Wilmsen et al., 2010). When evaluating the polygon distributions yielded by our model, we found them in agreement with the data (supplementary material Fig. S4B).

Parameter analysis

In order to assess the effect of the 33 model parameters, we doubled and halved the values of each of them, respectively, and simulated the wild type as well as the different experimental situations (supplementary material Tables S4-S7). This analysis reveals that most experimental results are reproduced by most parameter combinations, but that only a few combinations reproduce all of the results.

Experimental test of a model prediction

Our model predicts the formation of cell shape patterns over time. Akin to the compression gradient, it predicts the absence of a cell area gradient at the beginning of growth, followed by the formation of a cell area gradient with small cells in the center of the disc. Subsequently, this cell area gradient is predicted to become shallower.

In order to test this prediction experimentally, we had to take into account the three-dimensional shape of the wing pouch, as the pouch becomes curved as it grows. The analysis is complicated

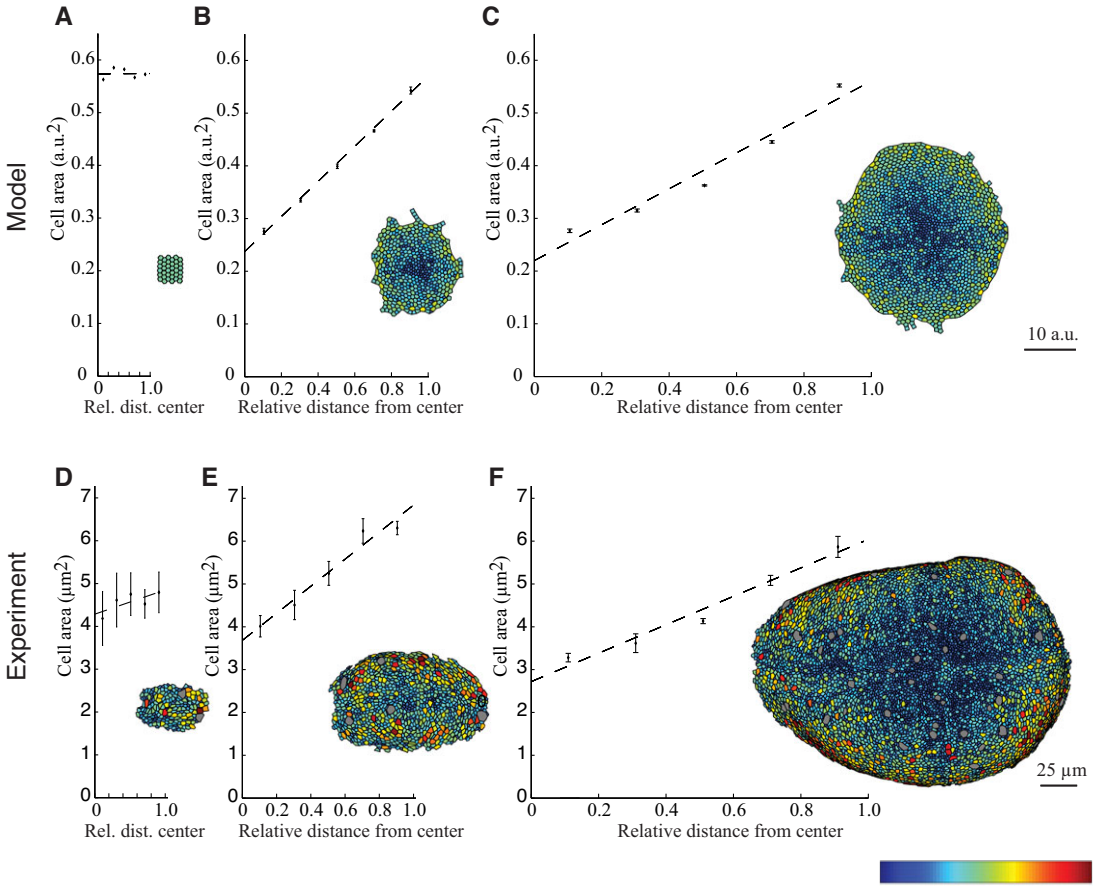

Fig. 6. Comparison of predicted and measured cell area distributions. (**A-C**) Our model predicts an initial build-up of a cell area gradient (A,B), which is flattened at later stages (C). (**D**,**F**) Initial conditions (A) are compared with wing discs in which the ring of *wg* expression has not yet formed (D), and final simulated distributions (C) are compared with late third instar discs (F). (**E**) The pouches of the mid third instar discs contain about one quarter the number of cells of those in the late third instar and are compared with simulated discs (B) that contain roughly the same factor-less cells than the final simulated disc. Average results ±s.e.m. of three discs are shown. Dotted lines are linear least square fits through the means. For better comparison of the different stages, the length of the *x*-axis was scaled with the square root of the area of the late respective discs. Cells were colored according to their area, ranging from 0 to 1.3 a.u.^{2} for the simulated and from 0 to 16 μm^2 for the experimental discs. Images were scaled such that the average cell areas of later simulated and experimental discs are approximately the same. Gray cells are in mitosis and were excluded from the analysis. The initial conditions of the model consist of hexagons only. In this case, cell areas obtained by the simulation are larger than in the case of irregular polygon numbers (~0.5 a.u.^{2}).

further by the presence of the peripodial membrane, a thin epithelial layer that lies on top of the wing pouch. We therefore further developed open source software in order to facilitate this analysis (supplementary material Fig. S1).

In order to assess whether there is initially no cell area gradient present, we analyzed discs in which the ring of *wg* expression has not yet formed. These discs show, on average, a shallow cell area gradient, but there is considerable variation (Fig. 6D). Two out of three discs do not show a significant positive correlation between relative distance from the center of the pouch and cell area (P=0.9 and P=1.0, respectively, Spearman's rank), whereas one disc does show a significant correlation (P<0.001). One of the former discs even shows a negative correlation (P<0.05). At the mid-third instar stage, the discs show a much steeper gradient (Fig. 6E) and there is indeed a highly significant correlation between relative distance from the center and cell area (P<10^{-5} for each disc). At the late third instar stage, the gradient is less steep (Fig. 6F), but the correlations are still highly significant (P<10^{-5} for each disc) and the variation among discs is smallest at this stage. Thus, the observed changes of the area gradient are similar to the ones predicted.

In addition to the formation of a cell area gradient, the model also predicts a concurrent tangential elongation of peripheral cells. As shown in supplementary material Fig. S5, the elongation direction of cells in young discs is almost random, whereas peripheral cells in later discs are preferentially elongated in the tangential direction. Even though the experimentally observed pattern seems to be more complex owing to the presence of compartment boundaries, the general trend in observed elongation directions is similar to that predicted.

DISCUSSION

We present a new model for the regulation of wing disc size. The model contains a rather complex regulatory network, which consists of a considerable number of interactions, receives non-uniform input of protein activities, and interacts with a mechanical stress pattern that emerges over time and space. Nevertheless, a qualitative understanding can be gained by considering it in terms of a compression gradient model. During growth, compression increases in the center of the disc. Growth ceases when compression in the center reaches a certain threshold and the

gradient of the compression gradient drops below a certain threshold in the rest of the disc. Read-out of the compression gradient is accomplished by a mechanism that involves Vg and the Hippo pathway. We have used numerical simulations to show that the model can account for growth termination and that it reproduces a large range of additional data on growth regulation, including some emergent properties of the system.

Based upon the principle underlying the model, predictions can be made with respect to cell shape patterns. In order to take into account the curved surface of the wing pouch, we further developed an open source image analysis program. Our results showed that the general dynamics of the formation of cell shape patterns is indeed similar to the one predicted by the model. This analysis is, however, based on images from different discs and, especially during the early stages, there is variation among discs. It would therefore be interesting to assess whether the predicted dynamics is also present in the temporal evolution of single discs. However, this first requires the development of experimental methods with which single discs can be followed over time.

Even though the development of cell shape patterns constitutes a fundamental prediction of the model, it would be an interesting future experimental challenge to test the model's basic assumptions directly, i.e. the regulation of Yki, Arm and *ds* by mechanical forces. The regulation of Yki by mechanical compression is most relevant for the model's behavior and appears necessary to obtain growth termination in combination with roughly uniform growth. The regulation of Arm by compression seems to be involved in stabilizing the Vg gradient, which could be relatively unstable if it would be regulated by Vg autoregulation alone. In addition, this interaction smoothens the compression gradient, which might have implications for the 3D structure of the wing disc. Last, the regulation of *ds* by mechanical forces is not essential for the principle behind size regulation, but improves the modeling results and also contributes to smoothening of the compression gradient.

While developing the model, we focused on its ability to reproduce specific features of growth dynamics, as well as a number of key experiments that are used to argue in favor and against current models. One of the latter results, the decrease of medial growth upon induction of uniform Dpp signaling, could not be reproduced (Rogulja and Irvine, 2005; Schwank et al., 2008). In the simulations, these discs grow very fast. It is conceivable that such growth rates cannot be sustained in vivo because of a limited availability of nutrients and oxygen. When imposing a maximum total growth rate on disc growth, it is indeed possible to obtain growth rates in the medial part that are lower than those in wild-type discs, whereas lateral growth rates are higher, in agreement with experiments (data not shown). Thus, with this additional assumption, the model can reproduce the results it was aimed to reproduce.

There are currently no experimental data available on the parameters underlying the model and therefore they were fitted manually. As has become clear from the parameter analysis, there are only a few parameter combinations that can reproduce all results. However, it is not known whether this set is reproduced robustly in vivo and there is no natural selection on reproducing experimental manipulations robustly. Nevertheless, it is entirely possible that a larger set of parameter values should reproduce the results. In addition, even though the model can reproduce the selected set of experimentally observed features, there are related observations it cannot reproduce. For example, the final size reached in the model is too small, the experimentally observed non-autonomous growth induction by clones overexpressing *brk* (Rogulja and Irvine, 2005) is nearly absent in our model, and growth induction along the boundary of *ds* overexpressing clones extends further inside the clone than measured experimentally. It would be interesting to study whether there are factors missing in the model, which would make the parameter space less strict. For example, the parameter space was strongly restricted by the stipulation to reproduce the absence of Vg-BE activity in ap^0 mutants upon ectopic *wg* expression. If it could be assumed that smaller discs have a different geometry in vivo than larger ones, the number of possible parameter combinations would increase. It will be interesting to assess the geometrical properties of discs in young larvae and evaluate whether the model should be adjusted in this respect.

Very recently, another model has been formulated for growth regulation that assumes that growth is regulated by increases of Dpp signaling levels over time (Wartlick et al., 2011). However, growth is increased in wing discs in which Brk and Dpp signaling are removed (Schwank et al., 2012). This either contradicts this model or the current understanding of Dpp signaling needs to be revised. Our model reproduces increased growth in such mutants, including its non-uniformity.

The adult wing is covered by bristles, which point towards the distal part of the wing. This orientation is regulated by planar polarity genes (McNeill, 2010). Regulation of planar polarity seems to be related to growth regulation. For example, Ds and Fj are not only important for growth regulation, but are also required for the development of a proximodistal polarity pattern (Adler et al., 1998; Zeidler et al., 2000). It is currently not clear whether Ds and Fj are directly involved in regulating planar polarity (Ma et al., 2003; Simon, 2004; Yang et al., 2002). If this were the case, then our model would suggest that planar polarity may, at least in part, arise from an interplay between morphogens and mechanical forces.

The model presented here was developed for the wing imaginal disc of *Drosophila*. It would be interesting to see whether a similar model could also reproduce size regulation and additional experimental results in other systems. For other imaginal discs, it has been shown that their centers are also compressed at the end of growth (Nienhaus et al., 2009). The precise regulatory networks involved in growth and size regulation are different for the different discs, but it would be interesting to see whether certain principles are conserved. In mammals, mechanical forces regulate growth in many tissues (Mammoto and Ingber, 2009). However, the situation is often very different from that in the wing disc in that most mammalian tissues reach their final size while they perform a biological function. Thus, it would be interesting to study whether principles similar to those described here apply for mammalian organs early during development.

Acknowledgements
We thank the high-performance computing team of the informatics services at UZH, in particular Raphael Graf, for support with the parameter analysis; Maria Willecke and Sabine Schilling for useful discussions; Gerald Schwank and George Hausmann for their comments on the manuscript; and the Developmental Studies Hybridoma Bank for supplying antibodies.

Funding
We thank the Swiss National Science Foundation, the Roche Research Foundation, the Forschungskredit of UZH, and SystemsX.ch within the framework of the WingX and the Plant Growth RTD for funding.

Competing interests statement
The authors declare no competing financial interests.

Supplementary material

Supplementary material available online at
http://dev.biologists.org/lookup/suppl/doi:10.1242/dev.082800/-/DC1

References

Adler, P. N., Charlton, J. and Liu, J. (1998). Mutations in the cadherin superfamily member gene dachsous cause a tissue polarity phenotype by altering frizzled signaling. *Development* **125**, 959-968.

Aegerter-Wilmsen, T., Aegerter, C. M., Hafen, E. and Basler, K. (2007). Model for the regulation of size in the wing imaginal disc of Drosophila. *Mech. Dev.* **124**, 318-326.

Aegerter-Wilmsen, T., Smith, A. C., Christen, A. J., Aegerter, C. M., Hafen, E. and Basler, K. (2010). Exploring the effects of mechanical feedback on epithelial topology. *Development* **137**, 499-506.

Asipauskas, M., Aubouy, M., Glazier, J., Graner, F. and Jiang, Y. (2003). A texture tensor to qualify deformations: the example of two-dimensional flowing foams. *Granul. Matter* **5**, 71-74.

Baena-López, L. A., Baonza, A. and García-Bellido, A. (2005). The orientation of cell divisions determines the shape of Drosophila organs. *Curr. Biol.* **15**, 1640-1644.

Baena-Lopez, L. A. and García-Bellido, A. (2006). Control of growth and positional information by the graded vestigial expression pattern in the wing of Drosophila melanogaster. *Proc. Natl. Acad. Sci. USA* **103**, 13734-13739.

Baonza, A. and Garcia-Bellido, A. (2000). Notch signaling directly controls cell proliferation in the Drosophila wing disc. *Proc. Natl. Acad. Sci. USA* **97**, 2609-2614.

Basler, K. and Struhl, G. (1994). Compartment boundaries and the control of Drosophila limb pattern by hedgehog protein. *Nature* **368**, 208-214.

Bittig, T., Wartlick, O., González-Gaitán, M. and Jülicher, F. (2009). Quantification of growth asymmetries in developing epithelia. *Eur. Phys. J. E Soft Matter* **30**, 93-99.

Bohn, H. (1976). Tissue interactions in the regenerating cockroach leg. In *Insect Development*, Vol. 8 (ed. P. Lawrence), pp. 170-185. Oxford, UK: Royal Entomological Society of London Symposium.

Bryant, P. J. and Levinson, P. (1985). Intrinsic growth control in the imaginal primordia of Drosophila, and the autonomous action of a lethal mutation causing overgrowth. *Dev. Biol.* **107**, 355-363.

Campbell, G. and Tomlinson, A. (1999). Transducing the Dpp morphogen gradient in the wing of Drosophila: regulation of Dpp targets by brinker. *Cell* **96**, 553-562.

Certel, K., Hudson, A., Carroll, S. B. and Johnson, W. A. (2000). Restricted patterning of vestigial expression in Drosophila wing imaginal discs requires synergistic activation by both Mad and the drifter POU domain transcription factor. *Development* **127**, 3173-3183.

Colombelli, J., Besser, A., Kress, H., Reynaud, E. G., Girard, P., Caussinus, E., Haselmann, U., Small, J. V., Schwarz, U. S. and Stelzer, E. H. (2009). Mechanosensing in actin stress fibers revealed by a close correlation between force and protein localization. *J. Cell Sci.* **122**, 1665-1679.

Couso, J. P., Bishop, S. A. and Martinez Arias, A. (1994). The wingless signalling pathway and the patterning of the wing margin in Drosophila. *Development* **120**, 621-636.

Couso, J. P., Knust, E. and Martinez Arias, A. (1995). Serrate and wingless cooperate to induce vestigial gene expression and wing formation in Drosophila. *Curr. Biol.* **5**, 1437-1448.

Day, S. J. and Lawrence, P. A. (2000). Measuring dimensions: the regulation of size and shape. *Development* **127**, 2977-2987.

Desprat, N., Supatto, W., Pouille, P. A., Beaurepaire, E. and Farge, E. (2008). Tissue deformation modulates twist expression to determine anterior midgut differentiation in Drosophila embryos. *Dev. Cell* **15**, 470-477.

Diaz-Benjumea, F. J. and Cohen, S. M. (1995). Serrate signals through Notch to establish a Wingless-dependent organizer at the dorsal/ventral compartment boundary of the Drosophila wing. *Development* **121**, 4215-4225.

Dupont, S., Morsut, L., Aragona, M., Enzo, E., Giulitti, S., Cordenonsi, M., Zanconato, F., Le Digabel, J., Forcato, M., Bicciato, S. et al. (2011). Role of YAP/TAZ in mechanotransduction. *Nature* **474**, 179-183.

Entchev, E. V., Schwabedissen, A. and González-Gaitán, M. (2000). Gradient formation of the TGF-beta homolog Dpp. *Cell* **103**, 981-992.

Farge, E. (2003). Mechanical induction of Twist in the Drosophila foregut/stomodeal primordium. *Curr. Biol.* **13**, 1365-1377.

Farhadifar, R., Röper, J. C., Aigouy, B., Eaton, S. and Jülicher, F. (2007). The influence of cell mechanics, cell-cell interactions, and proliferation on epithelial packing. *Curr. Biol.* **17**, 2095-2104.

Fernández, B. G., Gaspar, P., Brás-Pereira, C., Jezowska, B., Rebelo, S. R. and Janody, F. (2011). Actin-Capping Protein and the Hippo pathway regulate F-actin and tissue growth in Drosophila. *Development* **138**, 2337-2346.

French, V., Bryant, P. J. and Bryant, S. V. (1976). Pattern regulation in epimorphic fields. *Science* **193**, 969-981.

Gibson, M. C., Patel, A. B., Nagpal, R. and Perrimon, N. (2006). The emergence of geometric order in proliferating metazoan epithelia. *Nature* **442**, 1038-1041.

Go, M. J., Eastman, D. S. and Artavanis-Tsakonas, S. (1998). Cell proliferation control by Notch signaling in Drosophila development. *Development* **125**, 2031-2040.

Goulev, Y., Fauny, J. D., Gonzalez-Marti, B., Flagiello, D., Silber, J. and Zider, A. (2008). SCALLOPED interacts with YORKIE, the nuclear effector of the hippo tumor-suppressor pathway in Drosophila. *Curr. Biol.* **18**, 435-441.

Halder, G., Polaczyk, P., Kraus, M. E., Hudson, A., Kim, J., Laughon, A. and Carroll, S. (1998). The Vestigial and Scalloped proteins act together to directly regulate wing-specific gene expression in Drosophila. *Genes Dev.* **12**, 3900-3909.

Huang, J., Wu, S., Barrera, J., Matthews, K. and Pan, D. (2005). The Hippo signaling pathway coordinately regulates cell proliferation and apoptosis by inactivating Yorkie, the Drosophila homolog of YAP. *Cell* **122**, 421-434.

Hufnagel, L., Teleman, A. A., Rouault, H., Cohen, S. M. and Shraiman, B. I. (2007). On the mechanism of wing size determination in fly development. *Proc. Natl. Acad. Sci. USA* **104**, 3835-3840.

Jazwinska, A., Kirov, N., Wieschaus, E., Roth, S. and Rushlow, C. (1999). The Drosophila gene brinker reveals a novel mechanism of Dpp target gene regulation. *Cell* **96**, 563-573.

Jursnich, V. A., Fraser, S. E., Held, L. I., Jr, Ryerse, J. and Bryant, P. J. (1990). Defective gap-junctional communication associated with imaginal disc overgrowth and degeneration caused by mutations of the dco gene in Drosophila. *Dev. Biol.* **140**, 413-429.

Kasza, K. E. and Zallen, J. A. (2011). Dynamics and regulation of contractile actin-myosin networks in morphogenesis. *Curr. Opin. Cell Biol.* **23**, 30-38.

Kierzkowski, D., Nakayama, N., Routier-Kierzkowska, A. L., Weber, A., Bayer, E., Schorderet, M., Reinhardt, D., Kuhlemeier, C. and Smith, R. S. (2012). Elastic domains regulate growth and organogenesis in the plant shoot apical meristem. *Science* **335**, 1096-1099.

Kim, J., Irvine, K. D. and Carroll, S. B. (1995). Cell recognition, signal induction, and symmetrical gene activation at the dorsal-ventral boundary of the developing Drosophila wing. *Cell* **82**, 795-802.

Kim, J., Sebring, A., Esch, J. J., Kraus, M. E., Vorwerk, K., Magee, J. and Carroll, S. B. (1996). Integration of positional signals and regulation of wing formation and identity by Drosophila vestigial gene. *Nature* **382**, 133-138.

Kim, J., Johnson, K., Chen, H. J., Carroll, S. and Laughon, A. (1997). Drosophila Mad binds to DNA and directly mediates activation of vestigial by Decapentaplegic. *Nature* **388**, 304-308.

Kirkpatrick, H., Johnson, K. and Laughon, A. (2001). Repression of Dpp targets by binding of brinker to mad sites. *J. Biol. Chem.* **276**, 18216-18222.

Klein, T. and Arias, A. M. (1998). Different spatial and temporal interactions between Notch, wingless, and vestigial specify proximal and distal pattern elements of the wing in Drosophila. *Dev. Biol.* **194**, 196-212.

Lele, T. P., Pendse, J., Kumar, S., Salanga, M., Karavitis, J. and Ingber, D. E. (2006). Mechanical forces alter zyxin unbinding kinetics within focal adhesions of living cells. *J. Cell. Physiol.* **207**, 187-194.

Ma, D., Yang, C. H., McNeill, H., Simon, M. A. and Axelrod, J. D. (2003). Fidelity in planar cell polarity signalling. *Nature* **421**, 543-547.

Mammoto, A. and Ingber, D. E. (2009). Cytoskeletal control of growth and cell fate switching. *Curr. Opin. Cell Biol.* **21**, 864-870.

Mao, Y., Rauskolb, C., Cho, E., Hu, W. L., Hayter, H., Minihan, G., Katz, F. N. and Irvine, K. D. (2006). Dachs: an unconventional myosin that functions downstream of Fat to regulate growth, affinity and gene expression in Drosophila. *Development* **133**, 2539-2551.

Mao, Y., Tournier, A. L., Bates, P. A., Gale, J. E., Tapon, N. and Thompson, B. J. (2011). Planar polarization of the atypical myosin Dachs orients cell divisions in Drosophila. *Genes Dev.* **25**, 131-136.

Martín, F. A., Pérez-Garijo, A., Moreno, E. and Morata, G. (2004). The brinker gradient controls wing growth in Drosophila. *Development* **131**, 4921-4930.

McNeill, H. (2010). Planar cell polarity: keeping hairs straight is not so simple. *Cold Spring Harb. Perspect. Biol.* **2**, a003376.

Milán, M., Campuzano, S. and García-Bellido, A. (1996). Cell cycling and patterned cell proliferation in the wing primordium of Drosophila. *Proc. Natl. Acad. Sci. USA* **93**, 640-645.

Minami, M., Kinoshita, N., Kamoshida, Y., Tanimoto, H. and Tabata, T. (1999). brinker is a target of Dpp in Drosophila that negatively regulates Dpp-dependent genes. *Nature* **398**, 242-246.

Neumann, C. J. and Cohen, S. M. (1996a). Distinct mitogenic and cell fate specification functions of wingless in different regions of the wing. *Development* **122**, 1781-1789.

Neumann, C. J. and Cohen, S. M. (1996b). A hierarchy of cross-regulation involving Notch, wingless, vestigial and cut organizes the dorsal/ventral axis of the Drosophila wing. *Development* **122**, 3477-3485.

Neumann, C. J. and Cohen, S. M. (1997). Long-range action of Wingless organizes the dorsal-ventral axis of the Drosophila wing. *Development* **124**, 871-880.

Ng, M., Diaz-Benjumea, F. J., Vincent, J. P., Wu, J. and Cohen, S. M. (1996). Specification of the wing by localized expression of wingless protein. *Nature* **381**, 316-318.

Nienhaus, U., Aegerter-Wilmsen, T. and Aegerter, C. M. (2009). Determination of mechanical stress distribution in Drosophila wing discs using photoelasticity. *Mech. Dev.* **126**, 942-949.
Posakony, L. G., Raftery, L. A. and Gelbart, W. M. (1990). Wing formation in Drosophila melanogaster requires decapentaplegic gene function along the anterior-posterior compartment boundary. *Mech. Dev.* **33**, 69-82.
Rauskolb, C., Pan, G., Reddy, B. V., Oh, H. and Irvine, K. D. (2011). Zyxin links fat signaling to the hippo pathway. *PLoS Biol.* **9**, e1000624.
Resino, J., Salama-Cohen, P. and García-Bellido, A. (2002). Determining the role of patterned cell proliferation in the shape and size of the Drosophila wing. *Proc. Natl. Acad. Sci. USA* **99**, 7502-7507.
Rodríguez, I. (2004). The dachsous gene, a member of the cadherin family, is required for Wg-dependent pattern formation in the Drosophila wing disc. *Development* **131**, 3195-3206.
Rogulja, D. and Irvine, K. D. (2005). Regulation of cell proliferation by a morphogen gradient. *Cell* **123**, 449-461.
Rogulja, D., Rauskolb, C. and Irvine, K. D. (2008). Morphogen control of wing growth through the Fat signaling pathway. *Dev. Cell* **15**, 309-321.
Rulifson, E. J. and Blair, S. S. (1995). Notch regulates wingless expression and is not required for reception of the paracrine wingless signal during wing margin neurogenesis in Drosophila. *Development* **121**, 2813-2824.
Sansores-Garcia, L., Bossuyt, W., Wada, K., Yonemura, S., Tao, C., Sasaki, H. and Halder, G. (2011). Modulating F-actin organization induces organ growth by affecting the Hippo pathway. *EMBO J.* **30**, 2325-2335.
Schwank, G., Restrepo, S. and Basler, K. (2008). Growth regulation by Dpp: an essential role for Brinker and a non-essential role for graded signaling levels. *Development* **135**, 4003-4013.
Schwank, G., Tauriello, G., Yagi, R., Kranz, E., Koumoutsakos, P. and Basler, K. (2011). Antagonistic growth regulation by Dpp and Fat drives uniform cell proliferation. *Dev. Cell* **20**, 123-130.
Schwank, G., Yang, S. F., Restrepo, S. and Basler, K. (2012). Comment on "Dynamics of dpp signaling and proliferation control". *Science* **335**, 401.
Shraiman, B. I. (2005). Mechanical feedback as a possible regulator of tissue growth. *Proc. Natl. Acad. Sci. USA* **102**, 3318-3323.
Simon, M. A. (2004). Planar cell polarity in the Drosophila eye is directed by graded Four-jointed and Dachsous expression. *Development* **131**, 6175-6184.
Spencer, F. A., Hoffmann, F. M. and Gelbart, W. M. (1982). Decapentaplegic: a gene complex affecting morphogenesis in Drosophila melanogaster. *Cell* **28**, 451-461.
Strigini, M. and Cohen, S. M. (2000). Wingless gradient formation in the Drosophila wing. *Curr. Biol.* **10**, 293-300.
Tabata, T. and Kornberg, T. B. (1994). Hedgehog is a signaling protein with a key role in patterning Drosophila imaginal discs. *Cell* **76**, 89-102.
Teleman, A. A. and Cohen, S. M. (2000). Dpp gradient formation in the Drosophila wing imaginal disc. *Cell* **103**, 971-980.
Wada, K., Itoga, K., Okano, T., Yonemura, S. and Sasaki, H. (2011). Hippo pathway regulation by cell morphology and stress fibers. *Development* **138**, 3907-3914.
Wartlick, O., Mumcu, P., Kicheva, A., Bittig, T., Seum, C., Jülicher, F. and González-Gaitán, M. (2011). Dynamics of Dpp signaling and proliferation control. *Science* **331**, 1154-1159.
Willecke, M., Hamaratoglu, F., Sansores-Garcia, L., Tao, C. and Halder, G. (2008). Boundaries of Dachsous Cadherin activity modulate the Hippo signaling pathway to induce cell proliferation. *Proc. Natl. Acad. Sci. USA* **105**, 14897-14902.
Williams, J. A., Bell, J. B. and Carroll, S. B. (1991). Control of Drosophila wing and haltere development by the nuclear vestigial gene product. *Genes Dev.* **5**, 2481-2495.
Williams, J. A., Paddock, S. W. and Carroll, S. B. (1993). Pattern formation in a secondary field: a hierarchy of regulatory genes subdivides the developing Drosophila wing disc into discrete subregions. *Development* **117**, 571-584.
Williams, J. A., Paddock, S. W., Vorwerk, K. and Carroll, S. B. (1994). Organization of wing formation and induction of a wing-patterning gene at the dorsal/ventral compartment boundary. *Nature* **368**, 299-305.
Yang, C. H., Axelrod, J. D. and Simon, M. A. (2002). Regulation of Frizzled by fat-like cadherins during planar polarity signaling in the Drosophila compound eye. *Cell* **108**, 675-688.
Yoshigi, M., Hoffman, L. M., Jensen, C. C., Yost, H. J. and Beckerle, M. C. (2005). Mechanical force mobilizes zyxin from focal adhesions to actin filaments and regulates cytoskeletal reinforcement. *J. Cell Biol.* **171**, 209-215.
Zecca, M. and Struhl, G. (2007a). Control of Drosophila wing growth by the vestigial quadrant enhancer. *Development* **134**, 3011-3020.
Zecca, M. and Struhl, G. (2007b). Recruitment of cells into the Drosophila wing primordium by a feed-forward circuit of vestigial autoregulation. *Development* **134**, 3001-3010.
Zecca, M. and Struhl, G. (2010). A feed-forward circuit linking wingless, fat-dachsous signaling, and the warts-hippo pathway to Drosophila wing growth. *PLoS Biol.* **8**, e1000386.
Zecca, M., Basler, K. and Struhl, G. (1996). Direct and long-range action of a wingless morphogen gradient. *Cell* **87**, 833-844.
Zeidler, M. P., Perrimon, N. and Strutt, D. I. (2000). Multiple roles for four-jointed in planar polarity and limb patterning. *Dev. Biol.* **228**, 181-196.